

Sigma-Hole and Lone-Pair-Hole Site-Based Interactions of Seesaw Tetravalent Chalcogen-Bearing Molecules with Lewis Bases

Mahmoud A. A. Ibrahim,* Rehab R. A. Saeed, Mohammed N. I. Shehata, Nayra A. M. Moussa, Ahmed M. Tawfeek, Muhammad Naem Ahmed, Mohamed K. Abd El-Rahman, and Tamer Shoeb*



Cite This: *ACS Omega* 2023, 8, 32828–32837



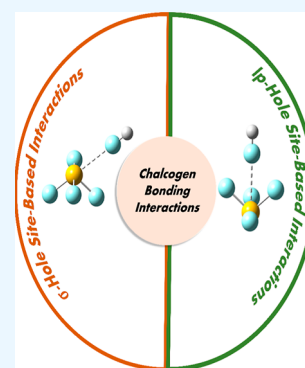
Read Online

ACCESS |

Metrics & More

Article Recommendations

ABSTRACT: For the first time, sigma (σ)- and lone-pair (lp)-hole site-based interactions of SF₄ and SeF₄ molecules in seesaw geometry with NH₃ and FH Lewis bases were herein comparatively investigated. The obtained findings from the electrostatic potential analysis outlined the emergence of sundry holes on the molecular entity of the SF₄ and SeF₄ molecules, dubbed the σ - and lp-holes. The energetic viewpoint announced splendid negative binding energy values for σ -hole site-based interactions succeeded by lp-hole analogues, which were found to be -9.21 and -0.50 kcal/mol, respectively, for SeF₄⋯NH₃ complex as a case study. Conspicuously, a proper concurrence between the strength of chalcogen σ -hole site-based interactions and the chalcogen's atomic size was obtained, whereas a reverse pattern was proclaimed for the lp-hole counterparts. Further, a higher preference for the YF₄⋯NH₃ complexes with elevated negative binding energy was promulgated over the YF₄⋯FH ones, indicating the eminent role of Lewis basicity. The indications of the quantum theory of atoms in molecules generally asserted the closed-shell nature of all the considered interactions. The observation of symmetry-adapted perturbation theory revealed the substantial contributing role of the electrostatic forces beyond the occurrence of σ -hole site-based interactions. In comparison, the dispersion forces were specified to govern the lp-hole counterparts. Such emerging findings would be a gate for the fruitful forthcoming applications of chalcogen bonding interactions in crystal engineering and biological systems.



1. INTRODUCTION

The electrostatic hole term was principally defined to be a region with scanty electron density over the surface of a chemical system.¹ In this respect, the emanating interactions of this electron-deficient region with the upcoming nucleophile were accordingly coined as “hole interactions”.^{1–4} These interactions embraced superior attention as an upshot to their prevalent contributions in a multitude of fields, including ligand–acceptor interactions,^{5,6} materials science,^{7–9} anion recognition,¹⁰ supramolecular chemistry,^{11–13} and drug discovery.^{14,15}

Chiefly, the hole sites were dissected into four categories on the ground of the covalent orbital origin. In detail, the σ -hole was illustrated to be an electron-deficient site located opposite to the covalent bond.^{2,16} Apparently, π -hole was announced to describe a perpendicular electron-deficient portion to a planar skeleton of a molecular system.^{17–20} Afterward, lone-pair (lp) hole was launched to be in the mirror to the lp position.^{21–23} Recently, radical (R[•]) hole was found in an opposite direction to the single electron (R[•]).²⁴ The electrophilic character of such holes enabled group IV–VIII elements to form spurious interactions with Lewis bases (LBs), dubbed as tetrel,^{25–27} pnictogen,^{28–33} chalcogen,^{34–39} halogen,^{40–44} and aerogen^{45–47} bonds, respectively.

A literature survey unveiled that manifold hole types could be simultaneously detected over the molecular entity of individual molecules, either on the same atom or different atoms over the molecular entity, regardless of the deformation effect. Despite announcing the presence of numerous holes over the entity of different atoms,^{24,48–53} the researchers triggered a precise inspection toward investigating the characteristics of sundry hole interactions over the surface of the same atom. Illustratively, the σ - and π -holes were thoroughly divulged over the aerogen atom of the KrF₂O and XeF₂O molecules.^{54,55} Whereas in the case of the ZF₃ (i.e., Z = N and P)⁵⁶ and XeO₃⁵⁷ molecules, σ - and lp-holes were comparatively inspected on the same atom. On the other hand, several studies demonstrated the opulent effect of the geometrical deformation on the σ -hole-containing molecules, which enabled the emergence of π -hole as in the case of ZF₂C₆H₅ (Z = P, As, Sb, Bi),⁵⁸ TF₄ (T = Si, Ge, Sn, Pb),⁵⁹ and YF₄ (Y = S, Se, Te, Po)⁶⁰ molecular systems. The obtained

Received: June 6, 2023

Accepted: July 21, 2023

Published: August 30, 2023



affirmations from those studies documented the higher preferentiality of σ -hole over the surface of the molecular systems to engage in interactions with LBs than other holes, either π -hole or lp-hole. However, the existence of lp-hole interactions within the seesaw geometry has not been elucidated yet. Accordingly, this research would evaluate a critical view of how receptive YF_4 molecules in seesaw geometry engage in chalcogen σ - and lp-hole site-based interactions with LB. In turn, the desired interactions were investigated in the fashion of $YF_4 \cdots LB$ (where $Y = S$ and Se ; $LB = NH_3$ and FH) complexes (see Figure 1). The emanating

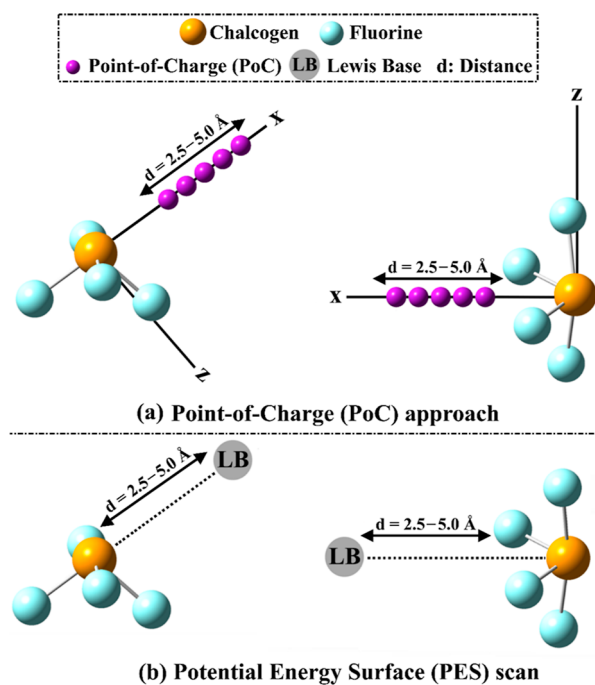


Figure 1. Graphical representation for (a) the PoC calculations for the YF_4 molecules (where $Y = S$ and Se) and (b) the PES scan for the scouted chalcogen σ - and lp-hole site-based interactions in the fashion of $YF_4 \cdots LB$ (where $LB = NH_3$ and FH) complexes.

findings within the presented work are intended to remove the mystery beyond the chalcogens' interaction origin and accordingly facilitate their analogue applications in organic chemistry, crystal engineering, and biological systems.

2. COMPUTATIONAL METHOD

The propensity of YF_4 molecules (i.e., $Y = S$ and Se) within the seesaw molecular geometry to be appealingly engaged in chalcogen σ - and lp-hole site-based interactions was minutely scrutinized and separately compared. In this vein, all the utilized chemical systems were geometrically optimized via the MP2/aug-cc-pVTZ level of theory other than the Se atom. The relativistic effects were considered for the latter atom using the pseudopotentials (PPs).^{61–64} To locate sites that are likely to be either nucleophilic or electrophilic, the electrostatic potential (EP) analyses were implemented by generating molecular EP (MEP) maps. The surface EP extrema ($V_{\sigma, \max}/V_{lp, \max}/V_{s, \min}$) values were afterward extracted. The 0.002 au electron density value was employed to perform EP calculations based on the earlier suggestions that confirmed its efficiency in representing the electron density distribution of the chemical systems.⁶⁵

To electrostatically investigate to what extent the SF_4 and SeF_4 molecules could favorably form chalcogen σ -^{66–68} and lp-hole⁵⁶ site-based interactions, the point-of-charge (PoC) approach was fulfilled. Thus, the Lewis basicity effect was inspected by employing PoCs of -0.25 and -0.50 au on the SF_4 and SeF_4 monomers through three different sites, namely the σ - and lp-holes. In accordance, the enumerated stabilization energy ($E_{\text{stabilization}}$) was quantified within the chalcogen σ - and lp-hole \cdots PoC distance scope of $2.5-5.0 \text{ \AA}$ through a 0.1 \AA step size using the following equation^{56,67,69}

$$E_{\text{stabilization}} = E_{\sigma\text{- and lp-hole-bearing molecule} \cdots \text{PoC}} - E_{\sigma\text{- and lp-hole-bearing molecule}} \quad (1)$$

The potential energy surface (PES) scan was applied to explicate the propensity of YF_4 molecules toward forming chalcogen σ - and lp-hole site-based interactions with the NH_3 and FH LBs. In this context, the optimized monomers were directed in three different orientations without permitting the distortion of the interacting monomers (see Figure 1). In the PES scan, the binding energy of $YF_4 \cdots LB$ complexes was evaluated at the MP2/aug-cc-pVTZ(PP) level of theory via chalcogen σ - and lp-hole \cdots LB distance scope ranged from 2.5 to 5.0 \AA through a 0.1 \AA step size. The binding energy of the considered complexes was evaluated as a result of the complex's energy minus the algebraic sum of the optimized monomers' energies. The counterpoise correction (CP) method was applied to eradicate the basis set superposition error (BSSE) from the obtained binding energies.⁷⁰ Benchmarking at the CCSD(T)/CBS level of theory was considered for the computed $E_{\text{MP2/aug-cc-pVTZ(PP)}}$ of the investigated complexes through the posterior equation.⁷¹

$$E_{\text{CCSD(T)/CBS}} = \Delta E_{\text{MP2/CBS}} + \Delta E_{\text{CCSD(T)}} \quad (2)$$

where

$$\Delta E_{\text{MP2/CBS}} = (64E_{\text{MP2/aug-cc-pVQZ(PP)}} - 27E_{\text{MP2/aug-cc-pVTZ(PP)}})/37 \quad (3)$$

$$\Delta E_{\text{CCSD(T)}} = E_{\text{CCSD(T)/aug-cc-pVDZ(PP)}} - E_{\text{MP2/aug-cc-pVDZ(PP)}} \quad (4)$$

In eqs 2–4, the MP2/aug-cc-pVQZ(PP), MP2/aug-cc-pVDZ(PP), and CCSD(T)/aug-cc-pVDZ(PP) levels of theory were employed to assess the $E_{\text{MP2/aug-cc-pVQZ(PP)}}$, $E_{\text{MP2/aug-cc-pVDZ(PP)}}$, and $E_{\text{CCSD(T)/aug-cc-pVDZ(PP)}}$, respectively.

In order to offer descriptive insight into the bonding characteristics of the scouted complexes, the quantum theory of atoms in molecules (QTAIM),⁷² along with the noncovalent interaction (NCI) index, were introduced.⁷³ Gaussian 09 software was utilized in order to accomplish all computations.⁷⁴ The analyses of EP, QTAIM, and NCI were performed with the help of Multiwfn 3.7 software.⁷⁵ The QTAIM schemes and NCI plots were conceived using the Visual Molecular Dynamics (VMD) program.⁷⁶ All the executed quantum mechanical computations were carried out using the MP2/aug-cc-pVTZ(PP) level of theory.

To quantitatively clarify the nature of the scouted interactions for the explored complexes, the symmetry-adapted perturbation theory (SAPT) was fulfilled.⁷⁷ In this spirit, total energy (E_{SAPT2}) was computed via eq 5,⁷⁸ in which it was

dissected into its constituent parts, namely dispersion (E_{disp}), exchange (E_{exch}), induction (E_{ind}), and electrostatic (E_{elst}), terms. The SAPT2 level of truncation incorporating the aug-cc-pVTZ basis set was employed using the PSI4 code.⁷⁹

$$E_{\text{SAPT2}} = E_{\text{elst}} + E_{\text{ind}} + E_{\text{disp}} + E_{\text{exch}} \quad (5)$$

where

$$E_{\text{elst}} = E_{\text{elst}}^{(10)} + E_{\text{elst},r}^{(12)} \quad (6)$$

$$E_{\text{ind}} = E_{\text{ind},r}^{(20)} + E_{\text{exch-ind},r}^{(20)} + E_{\text{ind}}^{(22)} + E_{\text{exch-ind}}^{(22)} + \delta E_{\text{HF},r}^{(2)} \quad (7)$$

$$E_{\text{disp}} = E_{\text{disp}}^{(20)} + E_{\text{exch-disp}}^{(20)} \quad (8)$$

$$E_{\text{exch}} = E_{\text{exch}}^{(10)} + E_{\text{exch}}^{(11)} + E_{\text{exch}}^{(12)} \quad (9)$$

3. RESULTS AND DISCUSSION

3.1. EP Analyses. EP was incorporated to minutely elucidate the possible bonding sites over entities of the chemical systems.^{80,81} Figure 2 displays the extracted MEP maps accompanied by the assessed $V_{\sigma,\text{max}}/V_{\text{lp,max}}$ and $V_{s,\text{min}}$ values for the YF_4 and LBs, respectively.

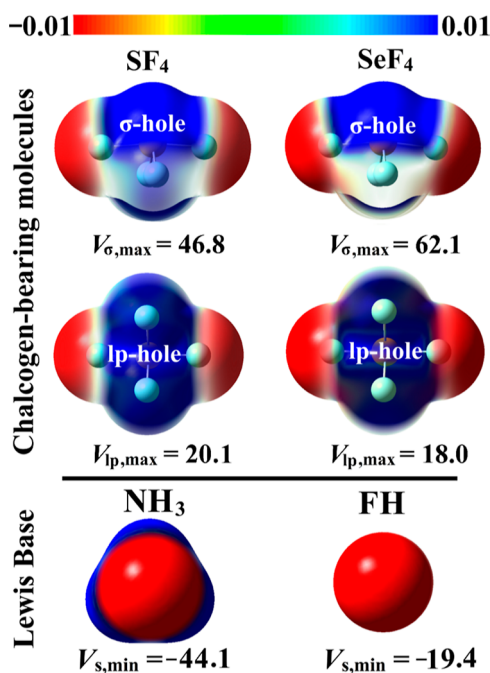


Figure 2. MEP maps of the σ - and lp-holes over the surface of the YF_4 molecules (where $\text{Y} = \text{S}$ and Se) along with the NH_3 and FH LBs. The EP aligned in the +0.01 au (blue) and -0.01 au (red) ambit. The $V_{\sigma,\text{max}}/V_{\text{lp,max}}/V_{s,\text{min}}$ values are in kcal/mol.

Looking at Figure 2, various blue-colored regions with distinct locations and sizes were observed over the molecular entities of the SF_4 and SeF_4 monomers. In line with literature relevant to the SF_4 and SeF_4 systems in seesaw geometry,³⁶ the most apparent area with a scanty electron density was discerned along the outer surface of the $\text{Y}-\text{F}$ bond (i.e., σ -hole). As well, a blue-colored region was perceived in opposite to the lp position of Y atom (i.e., lp-hole).

Comparatively, the obtained holes relevant to the YF_4 molecules were found with a resurgent magnitude as follows: lp-hole < σ -hole, for example, reputable positive EP with values

of 18.0 and 62.1 kcal/mol was detected over the lp- and σ -holes of the SeF_4 system, respectively. Further, σ -hole size was perceived to augment synchronically to the chalcogens' atomic size, and vice versa was obtained for the lp-hole. Turning to the LBs, the NH_3 and FH molecules were detected with red-coded regions surrounding their molecular structure and announced higher preferential $V_{s,\text{min}}$ upshots for the NH_3 compared to FH one, amounting to -44.1 and -19.4 kcal/mol, respectively.

3.2. PoC Calculations. Utilizing the PoC approach, the inclination of chemical systems to electrostatically interact with LBs via σ -, π -,⁶⁹ and lp-holes⁵⁶ was assessed. In this context, the chalcogen σ - and lp-hole...PoC distance impact was herein accomplished using a distance ranging from 2.5 to 5.0 Å through a 0.1 Å step size where PoC = -0.25 and -0.50 au. Figure 3 displays the stabilization energy curves. Table 1 compiles the stabilization energy ($E_{\text{stabilization}}$) computed at chalcogen σ -, π -, and lp-hole...PoC distance of 2.5 Å.

As demonstrated in Figure 3, the obtained negative $E_{\text{stabilization}}$ for all the YF_4 ...PoC systems declared preferential versatility of chalcogen σ - and lp-hole to electrostatically interact with negative PoCs (i.e., LBs). Notably, the stabilization energy curves outlined that the $E_{\text{stabilization}}$ was inversely correlated with the chalcogen σ - and lp-hole...PoC distance, respectively.

The numerical data summarized in Table 1 proclaimed that all the YF_4 ...PoC systems were discerned with elevated $E_{\text{stabilization}}$ values as follows: lp- < σ -hole. For instance, $E_{\text{stabilization}}$ values of the SeF_4 ...PoC system at the σ - and lp-hole...PoC under the -0.25 au PoC impact were -8.31 and -2.74 kcal/mol, respectively. Further, the PoC energetic upshots exposed the synchronicity of the $E_{\text{stabilization}}$ with chalcogen's atomic size for σ -hole site, whereas the reverse was detected for the lp-hole one. Quantitatively, $E_{\text{stabilization}}$ values of the SF_4 ... and SeF_4 ...PoC systems at chalcogen σ -/lp-hole...PoC, under the PoC influence of -0.25 au, were -5.49/-3.49 and -8.31/-2.74 kcal/mol, respectively. Eminently, higher negative PoCs led to ameliorated $E_{\text{stabilization}}$ values, affirming the preferable role of the Lewis basicity. For example, $E_{\text{stabilization}}$ values of the SeF_4 ...PoC system at σ -hole...PoC under the -0.50 and -0.25 au PoCs impact were -18.39 and -8.31 kcal/mol, respectively.

3.3. PES Scan. The PES scan was herein applied in order to provide an energetic assessment for chalcogen σ - and lp-hole site-based interactions of SF_4 and SeF_4 molecules in the seesaw geometrical structure with the NH_3 and FH LBs. Accordingly, binding energy was computed for the YF_4 ...LB complexes at chalcogen σ - and lp-hole...LB distance ranging from 2.5 to 5.0 Å through a 0.1 Å step size. The PES scan graphs of YF_4 ... NH_3 / FH complexes were generated and are illustrated in Figure 4. Upon the most proficient distances, binding energy was benchmarked at the CCSD/CBS level of theory for the investigated complexes. Table 2 gathers the computed binding energy at all the studied levels of theories for the complexes under study.

All the YF_4 ...LB complexes exhibited preferential negative values of binding energy with disparate preferability (see Figure 4). This finding declared the propensity of the SF_4 and SeF_4 molecules to preferentially engage in the previously documented σ -hole site-based interactions,³⁶ along with the unconventional lp-hole analogues.

With respect to the σ -hole site-based interaction, binding energy was perceived to be enhanced synchronically to the σ -hole size of the S and Se atoms, which aligned with the anterior

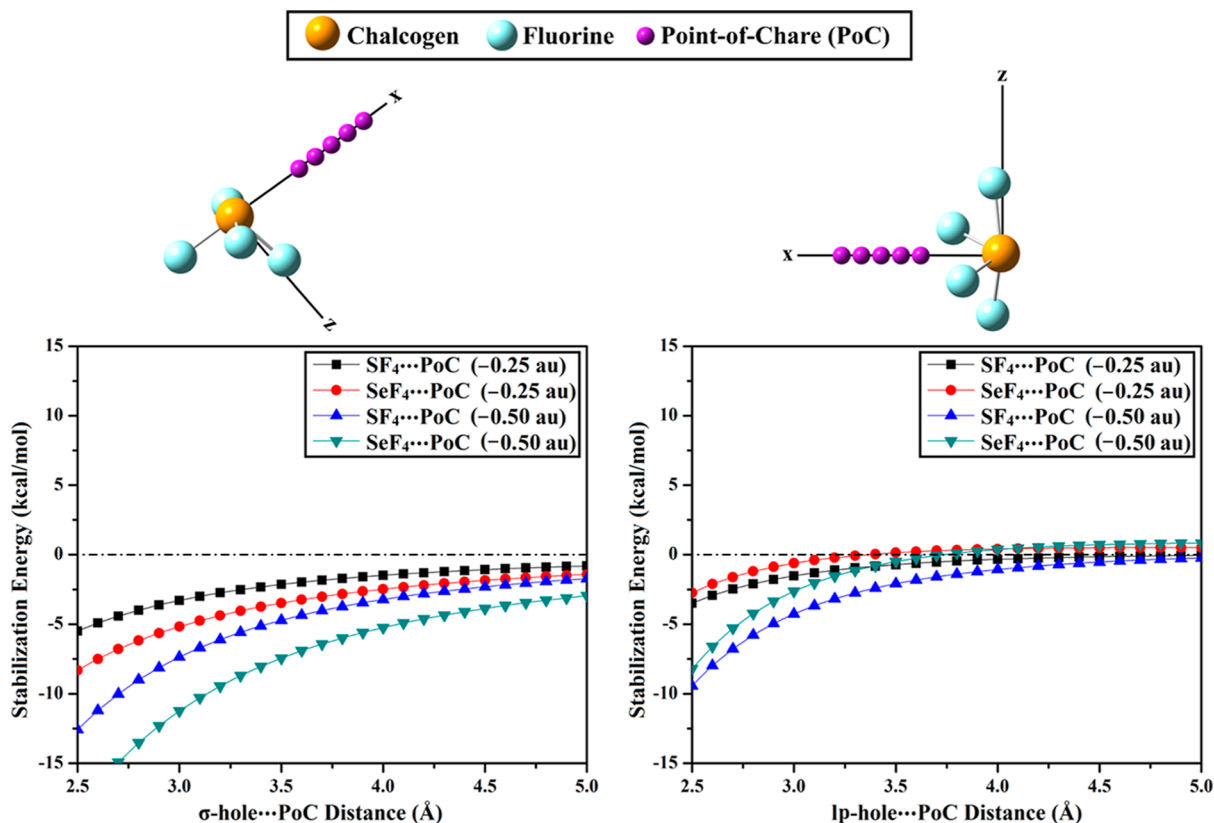


Figure 3. Stabilization energy curves for the examined $YF_4 \cdots PoC$ systems (where $Y = S$ and Se) within chalcogen σ - and lp-hole $\cdots PoC$ distance ranging from 2.5 to 5.0 Å influenced by PoCs = -0.25 and -0.50 au.

Table 1. $E_{\text{stabilization}}$ of the $YF_4 \cdots PoC$ Systems (Where $Y = S$ and Se) at Chalcogen σ - and lp-Hole $\cdots PoC$ Distance of 2.5 Å and PoCs = -0.25 and -0.50 au

site	stabilization energy ($E_{\text{stabilization}}$, kcal/mol)			
	PoC = -0.25 au		PoC = -0.50 au	
	SF ₄	SeF ₄	SF ₄	SeF ₄
σ -hole	-5.49	-8.31	-12.56	-18.39
lp-hole	-3.49	-2.74	-9.43	-8.20

studies.³⁶ Illustratively, paramount negative $E_{MP2/aug-cc-pVTZ(PP)}$ values of -5.38 and -9.21 kcal/mol were denoted for the SF₄ \cdots and SeF₄ \cdots NH₃ complexes, respectively. On the contrary, for the lp-hole site-based interactions, the energetic observations announced superior binding energies for the sulfur-bearing complexes than the selenium-bearing ones, alluding to the lp-hole size. For instance, concerning the SF₄ \cdots and SeF₄ \cdots NH₃ complexes, $E_{MP2/aug-cc-pVTZ(PP)}$ were -0.83 and -0.50 kcal/mol versus positive EP values of 20.1 and 18.0 kcal/mol for SF₄ and SeF₄ molecules, respectively.

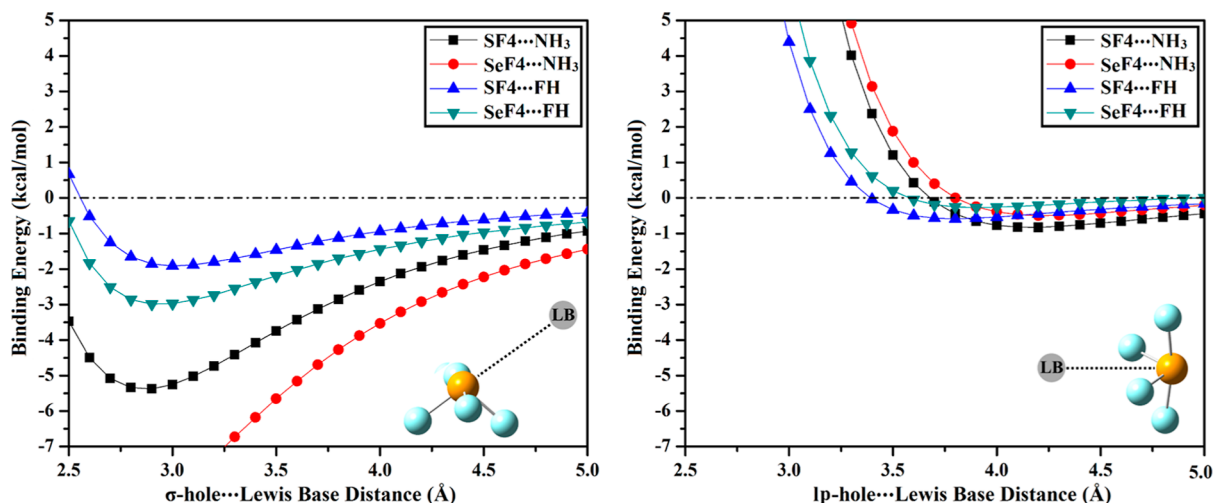


Figure 4. Binding energy curves of chalcogen σ - and lp-hole site-based interactions within $YF_4 \cdots NH_3/FH$ complexes (where $Y = S$ and Se) evaluated through chalcogen σ - and lp-hole $\cdots LB$ distance in a range of 2.5–5.0 Å.

Table 2. Binding Energies Calculated at the MP2/aug-cc-pVTZ(PP) and CCSD(T)/CBS for the Chalcogen σ - and lp-Hole Site-Based Interactions within the $YF_4 \cdots NH_3/FH$ Complexes (Where $Y = S$ and Se) at the Most Proficient Chalcogen σ - and lp-Hole \cdots Lewis Bases Distance (in Å)

complex	distance (Å) ^a	$E_{MP2/aug-cc-pVTZ(PP)}$ (kcal/mol)	$E_{CCSD(T)/CBS}$ (kcal/mol)
σ -hole site-based interactions			
$SF_4 \cdots NH_3$	2.87	−5.38	−5.50
$SeF_4 \cdots NH_3$	2.72	−9.21	−9.58
$SF_4 \cdots FH$	3.00	−1.91	−2.07
$SeF_4 \cdots FH$	2.94	−3.00	−3.29
lp-hole site-based interactions			
$SF_4 \cdots NH_3$	4.16	−0.83	−0.97
$SeF_4 \cdots NH_3$	4.23	−0.50	−0.64
$SF_4 \cdots FH$	3.80	−0.59	−0.68
$SeF_4 \cdots FH$	3.91	−0.27	−0.38

^aThe most proficient distance was determined according to the binding energy curves presented in Figure 4.

Moreover, the favorability of $YF_4 \cdots LB$ complexes was shown in the order $YF_4 \cdots NH_3 > \cdots FH$ complexes, highlighting the synchronicity of the inspected interactions with the obtained results of EP analysis. As an example, $E_{MP2/aug-cc-pVTZ(PP)}$ findings for the σ -hole site-based interactions within $SeF_4 \cdots NH_3/\cdots FH$ complexes were $−9.21/−3.00$ kcal/mol along with $V_{s,min}$ results, amounting to $−44.1/−19.4$ kcal/mol regarding the NH_3/FH LBs, respectively.

Comparatively, for all the studied complexes, preferential negative binding energy values were recorded for σ -hole site-based interactions as compared to the lp-hole counterparts, which coincide with the EP affirmations. Illustratively, $E_{MP2/aug-cc-pVTZ(PP)}$ values for chalcogen σ -/lp-hole site-based interactions within the $SeF_4 \cdots NH_3$ complex were $−9.21/−0.50$ kcal/mol against positive σ -/lp-hole EP amounts of $62.1/18.0$ kcal/mol for the SeF_4 monomer, respectively. Overall, the binding energy pattern was consistent with the PoC-based results. For instance, in lp-hole site-based interactions, the $SeF_4 \cdots NH_3$ and $\cdots FH$ complexes showed $E_{MP2/aug-cc-pVTZ(PP)}$ values of $−0.50$ and $−0.27$ kcal/mol, which were synchronic to $E_{stabilization}$ with values of the $−8.20$ and $−2.74$ kcal/mol for the $SeF_4 \cdots PoC$ systems in the presence of $−0.50$ and $−0.25$ au, respectively. Generally, the obtained energetic results at the CCSD(T)/CBS level of theory proclaimed a great harmonization and precision for the upshots relevant to the MP2/aug-cc-pVTZ analog (Table 2).

3.4. QTAIM Analysis. In order to unveil the intermolecular interaction characteristics, the QTAIM was invoked. Based on the QTAIM perspective, the BPs and BCPs were built and are depicted in Figure 5 for all the $SF_4 \cdots$ and $SeF_4 \cdots NH_3/FH$ complexes. Further, the ρ_b , $\nabla^2\rho_b$, and H_b topological properties were computed and are given in Table 3.

Regarding σ -hole site-based interactions, one BP and BCP were noticed between the chalcogen-bearing molecules and the corresponding LB (Figure 5). While two BPs and BCPs were detected between the interacted species within the lp-hole site-based interactions. These findings declared the remarkable contributions of the fluorine atoms to the overall lp-hole site-based interactions.

The closed shell nature of the inspected complexes was assured by the tiny values of ρ_b and remarkable values of $\nabla^2\rho_b$ and H_b with a positive sign, except for the $SeF_4 \cdots NH_3$ complex. Negative H_b values were denoted for the latter complex, accentuating its partially covalent nature. The ρ_b , $\nabla^2\rho_b$, and H_b trends were consistently synchronic with the binding energy values. Illustratively, for σ -hole site-based interactions, the ρ_b

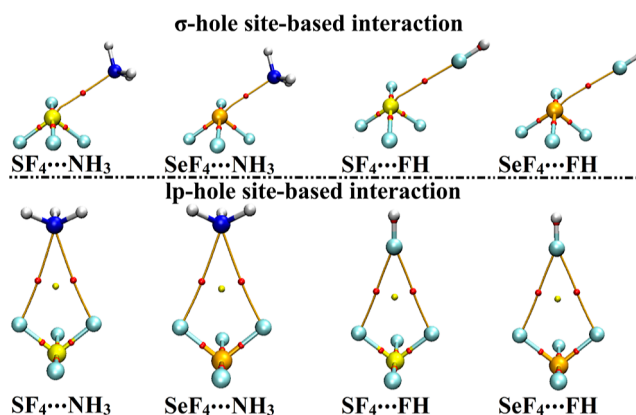


Figure 5. QTAIM diagrams for chalcogen σ - and lp-hole site-based interactions within the $YF_4 \cdots NH_3/FH$ complexes (where $Y = S$ and Se).

Table 3. ρ_b , $\nabla^2\rho_b$, and H_b Topological Parameters at BCPs for the Chalcogen σ - and lp-Hole Site-Based Interactions within the $YF_4 \cdots NH_3/FH$ Complexes (Where $Y = S$ and Se)

complex	ρ_b (au)	$\nabla^2\rho_b$ (au)	H_b (au)
σ -hole site-based interactions			
$SF_4 \cdots NH_3$	0.0201	0.0546	0.0006
$SeF_4 \cdots NH_3$	0.0298	0.0685	−0.0013
$SF_4 \cdots FH$	0.0082	0.0378	0.0018
$SeF_4 \cdots FH$	0.0105	0.0461	0.0019
lp-hole site-based interactions			
$SF_4 \cdots NH_3$	0.0036	0.0129	0.0007
$SeF_4 \cdots NH_3$	0.0035	0.0123	0.0006
$SF_4 \cdots FH$	0.0035	0.0179	0.0010
$SeF_4 \cdots FH$	0.0032	0.0160	0.0008

was found with values of 0.0201 and 0.0298 au (see Table 3) accompanied by $E_{MP2/aug-cc-pVTZ(PP)}$ amounting to $−5.38$ and $−9.21$, kcal/mol for the $SF_4 \cdots$ and $SeF_4 \cdots NH_3$ complexes, respectively.

3.5. NCI Analysis. NCI index was fulfilled to pictorially identify the nature of the interactions under inspection in a thoroughly descriptive way. In this vein, 2D reduced density gradient and 3D NCI plots were constructed to three-dimensionally illuminate whether the forces beyond the deemed complexes were attractive or repulsive force ones. NCI plots were perceived and are depicted for the $SF_4 \cdots$ and $SeF_4 \cdots NH_3/FH$ complexes in Figure 6.

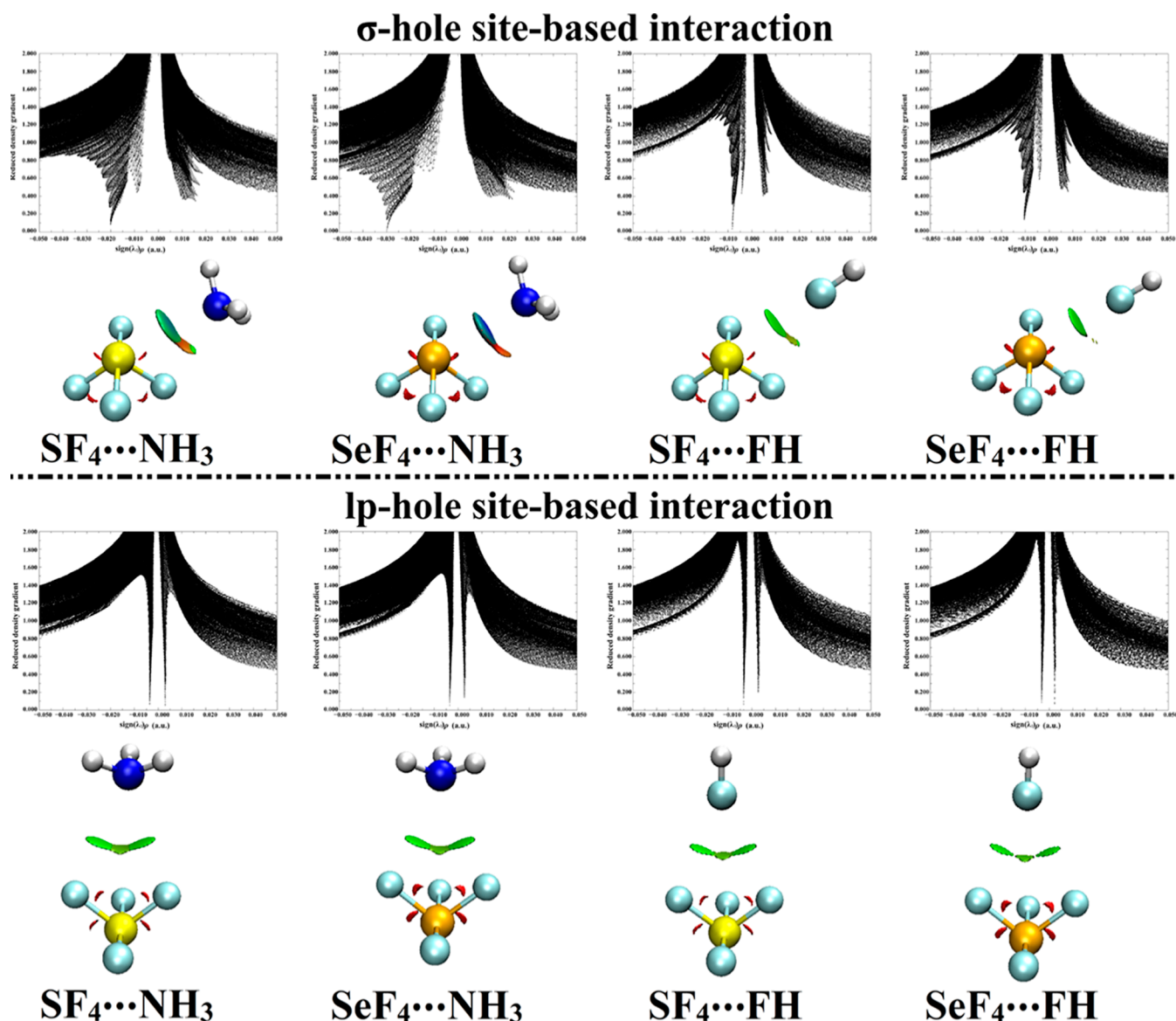


Figure 6. 2D and 3D NCI diagrams for chalcogen σ - and lp-hole site-based interactions within YF₄...NH₃/FH complexes (where Y = S and Se). The 2D plot isosurfaces are created using a value of 0.50 au. 3D NCI isosurfaces are mapped with a color scale ranging from blue to red depending on the $(\lambda_2)\rho$ sign between -0.035 and 0.020 au, respectively.

Table 4. E_{elst} , E_{disp} , E_{ind} , and E_{exch} , and E_{SAPT2} for the Chalcogen σ - and lp-Hole Site-Based Interactions within YF₄...NH₃/FH Complexes (Where Y = S and Se) with σ - and lp-hole...LB Most Proficient Distance

complex	E_{elst} (kcal/mol)	E_{disp} (kcal/mol)	E_{ind} (kcal/mol)	E_{exch} (kcal/mol)	E_{SAPT2} (kcal/mol) ^a	$\Delta\Delta E^b$
σ -hole site-based interactions						
SF ₄ ...NH ₃	-11.94	-4.10	-3.92	13.79	-6.17	0.79
SeF ₄ ...NH ₃	-19.51	-5.84	-8.28	23.54	-10.08	0.87
SF ₄ ...FH	-2.23	-1.40	-0.54	2.15	-2.03	0.12
SeF ₄ ...FH	-3.61	-1.72	-1.00	3.27	-3.06	0.06
lp-hole site-based interactions						
SF ₄ ...NH ₃	-1.06	-1.02	-0.21	1.35	-0.94	0.11
SeF ₄ ...NH ₃	-0.64	-1.04	-0.21	1.29	-0.60	0.10
SF ₄ ...FH	-0.39	-0.77	-0.10	0.66	-0.60	0.01
SeF ₄ ...FH	-0.04	-0.73	-0.10	0.57	-0.29	0.02

^a $E_{\text{SAPT2}} = E_{\text{elst}} + E_{\text{disp}} + E_{\text{ind}} + E_{\text{exch}}$, ^b $\Delta\Delta E = E_{\text{MP2/aug-cc-pVTZ(PP)}} - E_{\text{SAPT2}}$

Looking at Figure 6, 2D NCI plots displayed a clear shifting in the spikes toward negative $\text{sign}(\lambda_2)\rho$ values for all the examined complexes, affirming the existence of attractive forces

among the interacting species. Moreover, the green 3D NCI plots between the YF₄ molecules and the studied LBs conspicuously asserted the preferential attractive interactions

within the chalcogen σ - and lp-hole bearing complexes. Remarkably, the $\text{SeF}_4 \cdots \text{NH}_3$ complex announced a partially covalent nature, which was demonstrated through a blue-colored isosurfaces domain. Outstandingly, the variable-in-size green isosurfaces were denoted to be resurgent in the following sequence lp- < σ -hole site-based interactions, which was in line with the binding energy pattern. Concerning lp-hole site-based interactions, NCI plots supported the QTAIM claims, which declared the outstanding fluorine atoms' contributions (i.e., substituents) to the interactions within all the considered complexes.

3.6. SAPT Analysis. SAPT was herein devoted for a minute elucidation to the chalcogen σ - and lp-hole-based interactions' nature through subcategorizing the physical components of such interactions. In this regard, the energetic SAPT2 terms of $\text{SF}_4 \cdots$ and $\text{SeF}_4 \cdots \text{NH}_3/\text{FH}$ complexes are compiled in Table 4 and outlined in Figure 7.

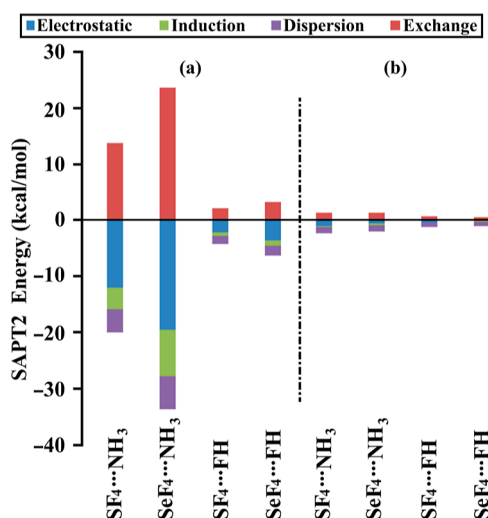


Figure 7. Bar chart illustrates the E_{SAPT2} components, comprising E_{elst} , E_{disp} , E_{ind} , and E_{exch} terms, for chalcogen (a) σ - and (b) lp-hole site-based interactions within $\text{YF}_4 \cdots \text{NH}_3/\text{FH}$ complexes (where $\text{Y} = \text{S}$ and Se).

The energetic components displayed in Figure 7 announced that E_{elst} , E_{disp} , and E_{ind} forces introduced an exemplary contribution to all chalcogen σ - and lp-hole site-based interactions within all investigated $\text{YF}_4 \cdots \text{LB}$ complexes, while the positive values of E_{exch} forces demonstrated their undesirable influence on all interactions' strength.

Upon the registered data in Table 4, regarding σ -hole site-based interactions, SAPT upshots announced the substantial contributions of the E_{elst} followed by E_{disp} and then E_{ind} forces for all investigated complexes. This could be interpreted as a result of the attractive electrostatic interactions between the positively charged area on the chalcogen atom and the negative clouds existing on the molecular surface of LBs. Numerically, in the case of the σ -hole site-based interaction within the $\text{SeF}_4 \cdots \text{NH}_3$ complex, the E_{elst} , E_{disp} , and E_{ind} energies were -11.94 , -4.10 , and -3.92 kcal/mol, respectively.

In comparison, regarding the lp-hole site-based interactions, the SAPT components were generally dominated in the order; $E_{\text{disp}} > E_{\text{elst}} > E_{\text{ind}}$ forces, respectively. For instance, $E_{\text{disp}}/E_{\text{elst}}/E_{\text{ind}}$ were $-1.04/-0.64/-0.21$ kcal/mol, for lp-hole site-based interactions within the $\text{SeF}_4 \cdots \text{NH}_3$ complex. The exactitude of the adopted SAPT calculations was established via nominal

energy difference ($\Delta\Delta E$ values) between the $E_{\text{MP2/aug-cc-pVTZ(PP)}}$ and SAPT2 energies. Generally, the negative energetic components (i.e., E_{elst} , E_{disp} , and E_{ind}) coincided with the binding energy pattern. Illustratively, for σ -hole site-based interactions, E_{elst} values were -19.51 and -3.61 kcal/mol accompanied with $E_{\text{MP2/aug-cc-pVTZ(PP)}}$ values of -9.21 and -3.00 kcal/mol for the $\text{SeF}_4 \cdots \text{NH}_3$ and $\cdots \text{FH}$ complexes.

4. CONCLUSIONS

In the current work, the potentiality of the YF_4 molecules (i.e., $\text{Y} = \text{S}$ and Se) within the seesaw molecular geometry to engage in chalcogen σ - and lp-hole site-based interactions with NH_3 and FH LBs was thoroughly disclosed. Conspicuously, the EP affirmations proclaimed the existence of σ - and lp-holes over the SF_4 and SeF_4 molecular entities. The energetic viewpoint declared more favorable binding energy values for the σ -hole site-based interactions than lp-hole ones within all inspected complexes. Moreover, the binding energy showed a parallel pattern to the chalcogens' atomic size within the σ -hole site-based interactions; however, a reverse concatenation was perceived for the lp-hole counterparts. The closed-shell nature of the studied interactions was assured via the QTAIM and NCI observations, except for the σ -hole site-based interaction within the $\text{SeF}_4 \cdots \text{NH}_3$ complex. Such σ -hole site-based interaction within the latter complex was disclosed with a partially covalent character. SAPT upshots accentuated that the E_{elst} was the main driving force for σ -hole site-based interactions, whilst the E_{disp} forces generally controlled the lp-hole ones. These findings would be the linchpin for future crystal engineering and biological system applications.

AUTHOR INFORMATION

Corresponding Authors

Mahmoud A. A. Ibrahim – Computational Chemistry Laboratory, Chemistry Department, Faculty of Science, Minia University, Minia 61519, Egypt; School of Health Sciences, University of KwaZulu-Natal, Durban 4000, South Africa; orcid.org/0000-0003-4819-2040; Email: m.ibrahim@compchem.net

Tamer Shoeib – Department of Chemistry, The American University in Cairo, New Cairo 11835, Egypt; orcid.org/0000-0003-3512-1593; Email: t.shoeib@aucegypt.edu

Authors

Rehab R. A. Saeed – Computational Chemistry Laboratory, Chemistry Department, Faculty of Science, Minia University, Minia 61519, Egypt

Mohammed N. I. Shehata – Computational Chemistry Laboratory, Chemistry Department, Faculty of Science, Minia University, Minia 61519, Egypt; orcid.org/0000-0002-3334-6070

Nayra A. M. Moussa – Computational Chemistry Laboratory, Chemistry Department, Faculty of Science, Minia University, Minia 61519, Egypt; orcid.org/0000-0003-3712-7710

Ahmed M. Tawfeek – Chemistry Department, College of Science, King Saud University, Riyadh 11451, Saudi Arabia; orcid.org/0000-0001-5893-8710

Muhammad Naem Ahmed – Department of Chemistry, The University of Azad Jammu and Kashmir, Muzaffarabad 13100, Pakistan

Mohamed K. Abd El-Rahman – Department of Chemistry and Chemical Biology, Harvard University, Cambridge, Massachusetts 02138, United States

Complete contact information is available at:
<https://pubs.acs.org/10.1021/acsomega.3c03981>

Author Contributions

M.A.A.I.: conceptualization, methodology, software, resources, project administration, supervision, and writing—review and editing. R.R.A.S.: data curation, formal analysis, investigation, visualization, and writing—original draft. M.N.I.S.: methodology, investigation, project administration, and writing—review and editing. N.A.M.M.: methodology, investigation, project administration, and writing—review and editing. A.M.T.: resources, and writing—review and editing. M.N.A.: visualization and writing—review and editing. M.K.A.E.-R.: writing—review and editing. T.S.: conceptualization, methodology, and writing—review and editing.

Notes

The authors declare no competing financial interest.

ACKNOWLEDGMENTS

The authors acknowledge the financial support through Researchers Supporting Project number (RSPD2023R672), King Saud University, Riyadh, Saudi Arabia. The computational work was completed with resources provided by the Science and Technology Development Fund (STDF-Egypt, grants no. 5480 and 7972), Bibliotheca Alexandrina (<http://hpc.bibalex.org>) and The American University in Cairo. M.A.A.I. extends his appreciation to the Academy of Scientific Research and Technology (ASRT, Egypt) for funding the Graduation Projects conducted at CompChem Lab, Egypt.

REFERENCES

- (1) Tarannam, N.; Shukla, R.; Kozuch, S. Yet another perspective on hole interactions. *Phys. Chem. Chem. Phys.* **2021**, *23*, 19948–19963.
- (2) Clark, T.; Hennemann, M.; Murray, J. S.; Politzer, P. Halogen bonding: the sigma-hole. *J. Mol. Model.* **2007**, *13*, 291–296.
- (3) Angarov, V.; Kozuch, S. On the σ , π and δ hole interactions: A molecular orbital overview. *New J. Chem.* **2018**, *42*, 1413–1422.
- (4) Solel, E.; Kozuch, S. On the Power of Geometry over Tetrel Bonds. *Molecules* **2018**, *23*, 2742.
- (5) Mani, D.; Arunan, E. The X–C \cdots π (X = F, Cl, Br, CN) Carbon Bond. *J. Phys. Chem. A* **2014**, *118*, 10081–10089.
- (6) Mahmoudi, G.; Bauza, A.; Amini, M.; Molins, E.; Mague, J. T.; Frontera, A. On the importance of tetrel bonding interactions in lead(II) complexes with (iso)nicotinohydrazide based ligands and several anions. *Dalton Trans.* **2016**, *45*, 10708–10716.
- (7) Vickaryous, W. J.; Herges, R.; Johnson, D. W. Arsenic-pi interactions stabilize a self-assembled As₂L₃ supramolecular complex. *Angew. Chem., Int. Ed. Engl.* **2004**, *43*, 5831–5833.
- (8) Muller-Dethlefs, K.; Hobza, P. Noncovalent interactions: a challenge for experiment and theory. *Chem. Rev.* **2000**, *100*, 143–168.
- (9) Wolters, L. P.; Schyman, P.; Pavan, M. J.; Jorgensen, W. L.; Bickelhaupt, F. M.; Kozuch, S. The many faces of halogen bonding: a review of theoretical models and methods. *Wiley Interdiscip. Rev.: Comput. Mol. Sci.* **2014**, *4*, 523–540.
- (10) Lim, J. Y. C.; Beer, P. D. Sigma-Hole Interactions in Anion Recognition. *Chem* **2018**, *4*, 731–783.
- (11) Uhlenheuer, D. A.; Petkau, K.; Brunsveld, L. Combining supramolecular chemistry with biology. *Chem. Soc. Rev.* **2010**, *39*, 2817–2826.
- (12) Smith, D. K. A supramolecular approach to medicinal chemistry: Medicine beyond the molecule. *J. Chem. Educ.* **2005**, *82*, 393–400.
- (13) Bauza, A.; Mooibroek, T. J.; Frontera, A. Non-covalent sp³ carbon bonding with ArCF₃ is analogous to CH-pi interactions. *Chem. Commun.* **2014**, *50*, 12626–12629.
- (14) Lu, Y.; Wang, Y.; Zhu, W. Nonbonding interactions of organic halogens in biological systems: Implications for drug discovery and biomolecular design. *Phys. Chem. Chem. Phys.* **2010**, *12*, 4543–4551.
- (15) Lu, Y.; Liu, Y.; Xu, Z.; Li, H.; Liu, H.; Zhu, W. Halogen bonding for rational drug design and new drug discovery. *Expert Opin. Drug Discovery* **2012**, *7*, 375–383.
- (16) Politzer, P.; Murray, J. S.; Clark, T.; Resnati, G. The sigma-hole revisited. *Phys. Chem. Chem. Phys.* **2017**, *19*, 32166–32178.
- (17) Novotny, J.; Bazzi, S.; Marek, R.; Kozelka, J. Lone-pair-pi interactions: analysis of the physical origin and biological implications. *Phys. Chem. Chem. Phys.* **2016**, *18*, 19472–19481.
- (18) Bauza, A.; Frontera, A.; Mooibroek, T. J. π -Hole Interactions Involving Nitro Aromatic Ligands in Protein Structures. *Chemistry* **2019**, *25*, 13436–13443.
- (19) Politzer, P.; Murray, J. S.; Clark, T. The pi-hole revisited. *Phys. Chem. Chem. Phys.* **2021**, *23*, 16458–16468.
- (20) Scheiner, S. Dissection of the Origin of pi-Holes and the Noncovalent Bonds in Which They Engage. *J. Phys. Chem. A* **2021**, *125*, 6514–6528.
- (21) Shukla, R.; Yu, D.; Mu, T.; Kozuch, S. Yet another perspective on hole interactions, part II: lp-hole vs lp-hole interactions. *Phys. Chem. Chem. Phys.* **2023**, *25*, 12641–12649.
- (22) Wang, C.; Danovich, D.; Shaik, S.; Wu, W.; Mo, Y. Attraction between electrophilic caps: A counterintuitive case of noncovalent interactions. *J. Comput. Chem.* **2019**, *40*, 1015–1022.
- (23) Del Bene, J. E.; Alkorta, I.; Elguero, J.; Sanchez-Sanz, G. Lone-Pair Hole on P: P–N Pnicogen Bonds Assisted by Halogen Bonds. *J. Phys. Chem. A* **2017**, *121*, 1362–1370.
- (24) Ibrahim, M. A. A.; Mohamed, Y. A. M.; Abd Elhafez, H. S. M.; Shehata, M. N. I.; Soliman, M. E. S.; Ahmed, M. N.; Abd El-Mageed, H. R.; Moussa, N. A. M. R^{*}-hole interactions of group IV–VII radical-containing molecules: A comparative study. *J. Mol. Graphics Modell.* **2022**, *111*, 108097.
- (25) Scheiner, S. Origins and properties of the tetrel bond. *Phys. Chem. Chem. Phys.* **2021**, *23*, 5702–5717.
- (26) Bhattarai, S.; Sutradhar, D.; Chandra, A. K. Strongly Bound pi-Hole Tetrel Bonded Complexes between H(2) SiO and Substituted Pyridines. Influence of Substituents. *ChemPhysChem* **2022**, *23*, No. e202200146.
- (27) Ibrahim, M. A. A.; Moussa, N. A. M.; Kamel, A. A. K.; Shehata, M. N. I.; Ahmed, M. N.; Taha, F.; Abourehab, M. A. S.; Shawky, A. M.; Elkaeed, E. B.; Soliman, M. E. S. External Electric Field Effect on the Strength of sigma-Hole Interactions: A Theoretical Perspective in Like . . . Like Carbon-Containing Complexes. *Molecules* **2022**, *27*, 2963.
- (28) Bauza, A.; Mooibroek, T. J.; Frontera, A. σ -Hole Opposite to a Lone Pair: Unconventional Pnicogen Bonding Interactions between ZF₃(Z=N, P, As, and Sb) Compounds and Several Donors. *ChemPhysChem* **2016**, *17*, 1608–1614.
- (29) Feng, G.; Evangelisti, L.; Gasparini, N.; Caminati, W. On the Cl–N halogen bond: a rotational study of CF₃Cl.NH₃. *Chemistry* **2012**, *18*, 1364–1368.
- (30) Murray, J. S.; Lane, P.; Politzer, P. A predicted new type of directional noncovalent interaction. *Int. J. Quantum Chem.* **2007**, *107*, 2286–2292.
- (31) Scheiner, S. The pnicogen bond: its relation to hydrogen, halogen, and other noncovalent bonds. *Acc. Chem. Res.* **2013**, *46*, 280–288.
- (32) Blanco, F.; Alkorta, I.; Rozas, I.; Solimannejad, M.; Elguero, J. A theoretical study of the interactions of NF(3) with neutral ambidentate electron donor and acceptor molecules. *Phys. Chem. Chem. Phys.* **2011**, *13*, 674–683.
- (33) Alkorta, I.; Elguero, J.; Del Bene, J. E. Exploring the PX₃:NCH and PX₃:NH₃ potential surfaces, with X = F, Cl, and Br. *Chem. Phys. Lett.* **2015**, *641*, 84–89.
- (34) Bhattarai, S.; Sutradhar, D.; Huyskens, T. Z.; Chandra, A. K. Nature and Strength of the π -Hole Chalcogen Bonded Complexes between Substituted Pyridines and SO₃ Molecule. *ChemistrySelect* **2021**, *6*, 7514–7524.

- (35) Azofra, L. M.; Scheiner, S. Substituent Effects in the Noncovalent Bonding of SO(2) to Molecules Containing a Carbonyl Group. The Dominating Role of the Chalcogen Bond. *J. Phys. Chem. A* **2014**, *118*, 3835–3845.
- (36) Scheiner, S.; Lu, J. Halogen, Chalcogen, and Pnicogen Bonding Involving Hypervalent Atoms. *Chem.—Eur. J.* **2018**, *24*, 8167–8177.
- (37) Varadwaj, P. R. Does Oxygen Feature Chalcogen Bonding? *Molecules* **2019**, *24*, 3166–3183.
- (38) Wang, W.; Ji, B.; Zhang, Y. Chalcogen bond: A sister noncovalent bond to halogen bond. *J. Phys. Chem. A* **2009**, *113*, 8132–8135.
- (39) Aakeroy, C. B.; Bryce, D. L.; Desiraju, G.; Frontera, A.; Legon, A. C.; Nicotra, F.; Rissanen, K.; Scheiner, S.; Terraneo, G.; Metrangolo, P.; Resnati, G. Definition of the chalcogen bond (IUPAC Recommendations 2019). *Pure Appl. Chem.* **2019**, *91*, 1889–1892.
- (40) Zhou, F.; Liu, Y.; Wang, Z.; Lu, T.; Yang, Q.; Liu, Y.; Zheng, B. A new type of halogen bond involving multivalent astatine: an ab initio study. *Phys. Chem. Chem. Phys.* **2019**, *21*, 15310–15318.
- (41) Bundhun, A.; Ramasami, P.; Murray, J. S.; Politzer, P. Trends in sigma-hole strengths and interactions of F3MX molecules (M = C, Si, Ge and X = F, Cl, Br, I). *J. Mol. Model.* **2013**, *19*, 2739–2746.
- (42) Priimagi, A.; Cavallo, G.; Metrangolo, P.; Resnati, G. The halogen bond in the design of functional supramolecular materials: recent advances. *Acc. Chem. Res.* **2013**, *46*, 2686–2695.
- (43) Politzer, P.; Lane, P.; Concha, M. C.; Ma, Y.; Murray, J. S. An overview of halogen bonding. *J. Mol. Model.* **2007**, *13*, 305–311.
- (44) Desiraju, G. R.; Ho, P. S.; Kloo, L.; Legon, A. C.; Marquardt, R.; Metrangolo, P.; Politzer, P.; Resnati, G.; Rissanen, K. Definition of the halogen bond (IUPAC Recommendations 2013). *Pure Appl. Chem.* **2013**, *85*, 1711–1713.
- (45) Bauza, A.; Frontera, A. π -Hole aerogen bonding interactions. *Phys. Chem. Chem. Phys.* **2015**, *17*, 24748–24753.
- (46) Esrafil, M. D.; Asadollahi, S.; Vakili, M. Investigation of substituent effects in aerogen-bonding interaction between ZO₃(Z=Kr, Xe) and nitrogen bases. *Int. J. Quantum Chem.* **2016**, *116*, 1254–1260.
- (47) Wang, R.; Liu, H.; Li, Q.; Scheiner, S. Xechalcogen aerogen bond. Effect of substituents and size of chalcogen atom. *Phys. Chem. Chem. Phys.* **2020**, *22*, 4115–4121.
- (48) Lang, T.; Li, X.; Meng, L.; Zheng, S.; Zeng, Y. The cooperativity between the σ -hole and π -hole interactions in the ClO \cdots XONO₂/XONO \cdots NH₃ (X = Cl, Br, I) complexes. *Struct. Chem.* **2014**, *26*, 213–221.
- (49) Solimannejad, M.; Nassirinia, N.; Amani, S. A computational study of 1:1 and 1:2 complexes of nitril halides (O₂NX) with HCN and HNC. *Struct. Chem.* **2012**, *24*, 651–659.
- (50) Solimannejad, M.; Ramezani, V.; Trujillo, C.; Alkorta, I.; Sanchez-Sanz, G.; Elguero, J. Competition and interplay between sigma-hole and pi-hole interactions: a computational study of 1:1 and 1:2 complexes of nitril halides (O₂NX) with ammonia. *J. Phys. Chem. A* **2012**, *116*, 5199–5206.
- (51) McDowell, S. A. C.; Joseph, J. A. A comparative study of model halogen-bonded, π -hole-bonded and cationic complexes involving NCX AND H₂O (X = F, Cl, Br). *Mol. Phys.* **2014**, *113*, 16–21.
- (52) Bauza, A.; Frontera, A. On the Versatility of BH(2) X (X=F, Cl, Br, and I) Compounds as Halogen-Hydrogen-and Triel-Bond Donors: An Ab Initio Study. *ChemPhysChem* **2016**, *17*, 3150–3186.
- (53) Alikhani, M. E. Beryllium bonding: insights from the sigma- and pi-hole analysis. *J. Mol. Model.* **2020**, *26*, 94.
- (54) Zierkiewicz, W.; Michalczyk, M.; Scheiner, S. Aerogen bonds formed between AeOF(2) (Ae = Kr, Xe) and diazines: comparisons between sigma-hole and pi-hole complexes. *Phys. Chem. Chem. Phys.* **2018**, *20*, 4676–4687.
- (55) Deng, Y.; Zanzhang, Cao, W.; Liu, Y.; Zheng, B.; Wang, Z. -Comparison of σ / π -hole aerogen-bonding interactions based on C2H₄ \cdots NgOX₂ (Ng = Kr, Xe; X = F, Cl, Br) complexes. *J. Mol. Model.* **2022**, *28*, 339.
- (56) Ibrahim, M. A. A.; Saad, S. M. A.; Al-Fahemi, J. H.; Mekhemer, G. A. H.; Ahmed, S. A.; Shawky, A. M.; Moussa, N. A. M. External electric field effects on the sigma-hole and lone-pair hole interactions of group V elements: a comparative investigation. *RSC Adv.* **2021**, *11*, 4022–4034.
- (57) Miao, J.; Xiong, Z.; Gao, Y. The effects of aerogen-bonding on the geometries and spectral properties of several small molecular clusters containing XeO(3). *J. Phys.: Condens. Matter* **2018**, *30*, 444001.
- (58) Zierkiewicz, W.; Michalczyk, M.; Wysokinski, R.; Scheiner, S. On the ability of pnicogen atoms to engage in both sigma and pi-hole complexes. Heterodimers of ZF(2)C(6)H(5) (Z = P, As, Sb, Bi) and NH(3). *J. Mol. Model.* **2019**, *25*, 152.
- (59) Michalczyk, M.; Zierkiewicz, W.; Wysokinski, R.; Scheiner, S. Hexacoordinated Tetrel-Bonded Complexes between TF(4) (T=Si, Ge, Sn, Pb) and NCH: Competition between sigma- and pi-Holes. *ChemPhysChem* **2019**, *20*, 959–966.
- (60) Zierkiewicz, W.; Wysokinski, R.; Michalczyk, M.; Scheiner, S. Chalcogen bonding of two ligands to hypervalent YF(4) (Y = S, Se, Te, Po). *Phys. Chem. Chem. Phys.* **2019**, *21*, 20829–20839.
- (61) Møller, C.; Plesset, M. S. Note on an approximation treatment for many-electron systems. *Phys. Rev.* **1934**, *46*, 618–622.
- (62) Woon, D. E.; Dunning, T. H. Gaussian basis sets for use in correlated molecular calculations. IV. Calculation of static electrical response properties. *J. Chem. Phys.* **1994**, *100*, 2975–2988.
- (63) Woon, D. E.; Dunning, T. H. Gaussian basis sets for use in correlated molecular calculations. III. The atoms aluminum through argon. *J. Chem. Phys.* **1993**, *98*, 1358–1371.
- (64) Feller, D. The role of databases in support of computational chemistry calculations. *J. Comput. Chem.* **1996**, *17*, 1571–1586.
- (65) Ibrahim, M. A. Molecular mechanical perspective on halogen bonding. *J. Mol. Model.* **2012**, *18*, 4625–4638.
- (66) Ibrahim, M. A. A.; Shehata, M. N. I.; Soliman, M. E. S.; Moustafa, M. F.; El-Mageed, H. R. A.; Moussa, N. A. M. Unusual chalcogen \cdots chalcogen interactions in like \cdots like and unlike Y=C=Y \cdots Y=C=Y complexes (Y = O, S, and Se). *Phys. Chem. Chem. Phys.* **2022**, *24*, 3386–3399.
- (67) Ibrahim, M. A. A.; Saeed, R. R. A.; Shehata, M. N. I.; Ahmed, M. N.; Shawky, A. M.; Khowdiary, M. M.; Elkaeed, E. B.; Soliman, M. E. S.; Moussa, N. A. M. Type I-IV Halogen-Halogen Interactions: A Comparative Theoretical Study in Halobenzene-Halobenzene Homodimers. *Int. J. Mol. Sci.* **2022**, *23*, 3114.
- (68) Ibrahim, M. A. A.; Shehata, M. N. I.; Rady, A. S. S. M.; Abuelliel, H. A. A.; Abd Elhafez, H. S. M.; Shawky, A. M.; Oraby, H. F.; Hasanin, T. H. A.; Soliman, M. E. S.; Moussa, N. A. M. Effects of Lewis Basicity and Acidity on sigma-Hole Interactions in Carbon-Bearing Complexes: A Comparative Ab Initio Study. *Int. J. Mol. Sci.* **2022**, *23*, 13023.
- (69) Ibrahim, M. A. A.; Saeed, R. R. A.; Shehata, M. N. I.; Mohamed, E. E. B.; Soliman, M. E. S.; Al-Fahemi, J. H.; El-Mageed, H. A.; Ahmed, M. N.; Shawky, A. M.; Moussa, N. A. M. Unexplored σ -hole and π -hole interactions in (X₂CY)₂ complexes (X = F, Cl; Y = O, S). *J. Mol. Struct.* **2022**, *1265*, 133232.
- (70) Boys, S. F.; Bernardi, F. The calculation of small molecular interactions by the differences of separate total energies. Some procedures with reduced errors. *Mol. Phys.* **2006**, *19*, 553–566.
- (71) Mishra, B. K.; Karthikeyan, S.; Ramanathan, V. Tuning the C–H \cdots π Interaction by Different Substitutions in Benzene–Acetylene Complexes. *J. Chem. Theory Comput.* **2012**, *8*, 1935–1942.
- (72) Bader, R. F. W. Atoms in molecules. *Acc. Chem. Res.* **1985**, *18*, 9–15.
- (73) Johnson, E. R.; Keinan, S.; Mori-Sanchez, P.; Contreras-Garcia, J.; Cohen, A. J.; Yang, W. Revealing noncovalent interactions. *J. Am. Chem. Soc.* **2010**, *132*, 6498–6506.
- (74) Frisch, M. J.; Trucks, G. W.; Schlegel, H. B.; Scuseria, G. E.; Robb, M. A.; Cheeseman, J. R.; Scalmani, G.; Barone, V.; Mennucci, B.; Petersson, G. A.; Nakatsuji, H.; Caricato, M.; Li, X.; Hratchian, H. P.; Izmaylov, A. F.; Bloino, J.; Zheng, G.; Sonnenberg, J. L.; Hada, M.; Ehara, M.; Toyota, K.; Fukuda, R.; Hasegawa, J.; Ishida, M.;

Nakajima, T.; Honda, Y.; Kitao, O.; Nakai, H.; Vreven, T.; Montgomery, J. A.; Peralta, J. E.; Ogliaro, F.; Bearpark, M.; Heyd, J. J.; Brothers, E.; Kudin, K. N.; Staroverov, V. N.; Kobayashi, R.; Normand, J.; Raghavachari, K.; Rendell, A.; Burant, J. C.; Iyengar, S. S.; Tomasi, J.; Cossi, M.; Rega, N.; Millam, J. M.; Klene, M.; Knox, J. E.; Cross, J. B.; Bakken, V.; Adamo, C.; Jaramillo, J.; Gomperts, R.; Stratmann, R. E.; Yazyev, O.; Austin, A. J.; Cammi, R.; Pomelli, C.; Ochterski, J. W.; Martin, R. L.; Morokuma, K.; Zakrzewski, V. G.; Voth, G. A.; Salvador, P.; Dannenberg, J. J.; Dapprich, S.; Daniels, A. D.; Farkas, Ö.; Foresman, J. B.; Ortiz, J. V.; Cioslowski, J.; Fox, D. J. *Gaussian 09*, Revision E01; Gaussian Inc.: Wallingford CT, USA, 2009.

(75) Lu, T.; Chen, F. Multiwfn: a multifunctional wavefunction analyzer. *J. Comput. Chem.* **2012**, *33*, 580–592.

(76) Humphrey, W.; Dalke, A.; Schulten, K. VMD: Visual molecular dynamics. *J. Mol. Graphics* **1996**, *14*, 33–38.

(77) Hohenstein, E. G.; Sherrill, C. D. Density fitting and Cholesky decomposition approximations in symmetry-adapted perturbation theory: Implementation and application to probe the nature of π - π interactions in linear acenes. *J. Chem. Phys.* **2010**, *132*, 184111–184120.

(78) Parker, T. M.; Burns, L. A.; Parrish, R. M.; Ryno, A. G.; Sherrill, C. D. Levels of symmetry adapted perturbation theory (SAPT). I. Efficiency and performance for interaction energies. *J. Chem. Phys.* **2014**, *140*, 094106.

(79) Turney, J. M.; Simmonett, A. C.; Parrish, R. M.; Hohenstein, E. G.; Evangelista, F. A.; Fermann, J. T.; Mintz, B. J.; Burns, L. A.; Wilke, J. J.; Abrams, M. L.; Russ, N. J.; Leininger, M. L.; Janssen, C. L.; Seidl, E. T.; Allen, W. D.; Schaefer, H. F.; King, R. A.; Valeev, E. F.; Sherrill, C. D.; Crawford, T. D. PSI4: An open-source ab initio electronic structure program. *Wiley Interdiscip. Rev.: Comput. Mol. Sci.* **2012**, *2*, 556–565.

(80) Weiner, P. K.; Langridge, R.; Blaney, J. M.; Schaefer, R.; Kollman, P. A. Electrostatic potential molecular surfaces. *Proc. Natl. Acad. Sci. U.S.A.* **1982**, *79*, 3754–3758.

(81) Murray, J. S.; Politzer, P. The electrostatic potential: An overview. *Wiley Interdiscip. Rev.: Comput. Mol. Sci.* **2011**, *1*, 153–163.